BNL-64734

CONF-970945--

Photochemical carbon dioxide reduction with metal complexes: Differences between cobalt and nickel macrocycles

Etsuko Fujita,[a] Bruce S. Brunschwig,[a] Diane Cabelli,[a] Mark W. Renner,[b] Lars R. Furenlid,[c] Tomoyuki Ogata,[a,d] Yuji Wada,[d] and Shozo Yanagida[d]

[a] Chemistry Department, [b] Department of Applied Science, and [c] National Synchrotron Light Source, Brookhaven National Laboratory, Upton, NY 11973-5000, USA, [d] Material and Life Science, Graduate School of Engineering, Osaka University, Suita, Osaka 565, Japan

1. INTRODUCTION

Problems related to increases of green house gases in the atmosphere and the depletion of fossil fuels have made the conversion of CO_2 into useful chemicals and fuels an important area of research. However, CO_2 reduction poses many scientific challenges. Despite intense interest in photochemical and electrochemical CO_2 reduction, the kinetics and mechanism of the reduction remain unclear in many systems.

A number of 14-membered tetraazamacrocyclic complexes serve as catalysts for photochemical and electrochemical CO_2 reduction. $[CoHMD(H_2O)](ClO_4)_2$ (HMD = 5,7,7,12,14,14-hexamethyl-1,4,8,11-tetraaza-cyclotetradeca-4,11-diene)[1,2] and $Ni(cyclam)Cl_2$ (cyclam = 1,4,8,11-tetraazacyclotetradecane)[3] have been used as electrocatalysts for the reduction of CO_2 in H_2O or aqueous CH_3CN. The ratio for CO/H_2 production is ~1 for $[CoHMD(H_2O)](ClO_4)_2$ and >100 for $Ni(cyclam)Cl_2$. Metal(I) complexes, metal(III) hydride complexes, and metallocarboxylates such as $[Ni^{III}(cyclam)(CO_2^{2-})]^+$ are postulated as intermediates in the electro- and photo-chemical CO_2 reduction.[4]

Our research focuses on mechanistic and kinetic studies of photochemical and electrochemical CO_2 reduction that involves metal complexes as catalysts. This work makes use of UV-vis, NMR, and FTIR spectroscopy, flash photolysis, pulse radiolysis, X-ray diffraction, XANES (X-ray absorption near-edge spectroscopy) and EXAFS (extended X-ray absorption fine structure). Here we summarize our research on photochemical carbon dioxide reduction with metal macrocycles.

2. NATURE OF Co-CO_2 ADDUCTS

We and others have characterized the interaction of low-spin d^8 $Co^{I}HMD^+$ with CO_2 in CH_3CN[5-9] and in H_2O.[10,11] Schmidt et al.[12] have characterized the binding thermodynamics as a function of organic solvent. The chiral N-H centers of the macrocycle give rise to two diastereomers, *N-rac* and *N-meso*. The CoL complexes are shown below.

The equilibration between the *N-rac-* and *N-meso* cobalt(II) isomers is slow in acidic aqueous and organic media, but equilibration of the two cobalt(I) isomers is relatively rapid ($>2 \times 10^{-3}$ s^{-1}) in CH_3CN.

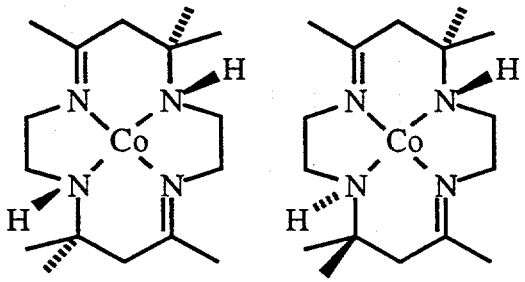

***rac* HMD** ***meso* HMD**

The CO_2 binding constants of the corresponding $[CoHMD]^+$ isomers are quite different: *N-rac*-$[CoHMD]^+$, $(1.2 \pm 0.5) \times 10^4$ M^{-1}; *N-meso*-$[CoHMD]^+$, 165 ± 15 M^{-1}.[5,6] While hydrogen bonding interactions between the bound CO_2 and amine protons of the macrocycle will tend to stabilize both adducts, the *N-meso* adduct is destabilized by the steric repulsion by the macrocycle methyl group.

Although the *N-rac*-$[CoHMD(CO_2)]^+$ adduct decomposes to *N-rac*-$[CoHMD]^{2+}$ and CO in wet CH_3CN,[5] it is stable enough to handle in dry CH_3CN under a CO_2 atmosphere. The complex is thermochromic,[6,7] being purple at room temperature and yellow at low temperature (–100 °C) as shown in Figure 1. The equilibrium between five-coordinate $[CoHMD(CO_2)]^+$ (purple) and six-coordinate $[CoHMD(CO_2)(CH_3CN)]^+$ (yellow) has been studied by UV-vis, ^1H NMR, FT-IR, XANES and EXAFS in CH_3CN.[6,7,9]

$$[CoHMD]^+ + CO_2 \rightleftharpoons [CoHMD(CO_2)]^+ \quad (1)$$

$$[CoHMD(CO_2)]^+ + CH_3CN \rightleftharpoons [CoHMD(CO_2)(CH_3CN)]^+ \quad (2)$$

$$K_s = [CoHMD(CO_2)(CH_3CN)^+] / [CoHMD(CO_2)^+] \quad (3)$$

The singular value decomposition (SVD)[13-15] spectral analysis of the temperature-dependent UV-vis data between 26 and -40 °C is consistent with the presence of two species in CH_3CN. The fit gives $\Delta H° = -7.0$ kcal mol^{-1} and $\Delta S° = -27$ cal K^{-1} mol^{-1} for eq. 2.[7] The equilibration is rapid on the NMR time scale. The pressure dependence of the equilibrium constant shows that increasing pressure shifts the equilibrium toward the six-coordinate species with an overall reaction volume of $\Delta V° = -17.7 \pm 1.0$ mL mol^{-1} at 15 C° in CH_3CN.[16] The FT-IR spectra measured over the range 25 to -75 °C in CD_3CN and in a CD_3CN/THF mixture indicates[7] the existence of four CO_2 adducts with and without intramolecular hydrogen bonds between the bound CO_2 and the amine hydrogens of the ligand: a five-coordinate, non-hydrogen-bonded form ($\nu_{C=O} = 1710$ cm^{-1}, $\nu_{NH} = 3208$ cm^{-1}), a five-coordinate hydrogen-bonded form ($\nu_{C=O} = 1626$ cm^{-1}), a six-coordinate non-hydrogen bonded form ($\nu_{C=O} = 1609$ cm^{-1}, $\nu_{NH} = 3224$ cm^{-1}), and a six-coordinate hydrogen-bonded form ($\nu_{C=O} = 1544$ cm^{-1}, $\nu_{NH} = 3145$ cm^{-1}).

DISCLAIMER

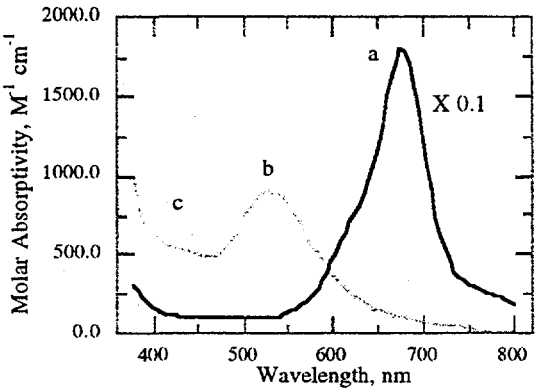

Figure 1. UV-vis spectra of $[Co^{I}HMD]^{+}$ (a), $[CoHMD(CO_2)]^{+}$ at room temperature (b), and $[Co^{III}HMD(CO_2^{2-})(CH_3CN)]^{+}$ at -100 C° (c) in CH_3CN.

X-ray absorption spectroscopy is an attractive tool for the characterization of metal complexes in solution. The metal coordination number, geometry, and electronic properties can be studied using XANES and the metal-ligand bond distances are obtained through analysis of EXAFS. Previous work[17-19] has also shown that the edge energy correlates with the oxidation state of the metal. The XANES spectra (Figure 2) for a series of CoHMD complexes[9] indicate that the edge positions (E_0) are sensitive to the oxidation state of the metal.

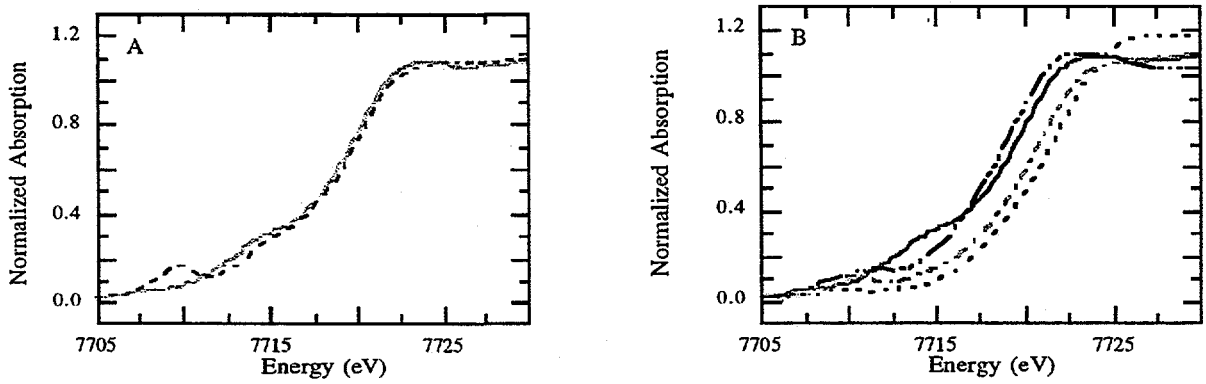

Figure 2. XANES spectra for a series of CoHMD complexes in various oxidation and ligation states. (A) $[Co^{II}HMD](ClO_4)_2$ in acetonitrile at 150 K (——), five-coordinate $[CoHMD(CO_2)]ClO_4$ in acetonitrile at room temperature (- - - -) (B) $[Co^{I}HMD(CO)]ClO_4$ in acetonitrile at room temperature (—— - - - - ——), $[Co^{II}HMD](ClO_4)_2$ in acetonitrile at 150 K (——), six-coordinate $[CH_3CN\text{-}CoHMD(CO_2)]ClO_4$ in acetonitrile at 150 K (—— - - ——) and $[Co^{III}HMD(CO_3^{2-})]ClO_4$ in H_2O at room temperature (- - - -).

The edge energy, relative to $[Co^{II}HMD]^{2+}$, decreases 1 eV upon reduction and increases 2 eV upon oxidation. As seen from Figure 2A, the E_0 for five-coordinate $[CoHMD(CO_2)]^+$ at room temperature is similar to that of $[Co^{II}HMD]^{2+}$. This is consistent with theoretical predictions[20,21] that the bound CO_2 receives 0.71 electrons mainly from the Co d_{z^2} orbital. The six-coordinate $[CoHMD(CO_2)(CH_3CN)]^+$ species shows a 1.2 eV shift towards Co(III) and is interpreted as a Co(III)-CO_2^{2-} carboxylate complex. Although the Co(III) carboxylates have been postulated as intermediates in CO_2 reduction and water-gas shift reactions, the XANES results provide the first unambiguous evidence that active metal catalysts, such as $[Co^{I}HMD]^+$, can promote two-electron transfer to the bound CO_2 and thereby facilitate its reduction.

3. PHOTOCHEMICAL CO_2 REDUCTION WITH COBALT MACROCYCLES: MECHANISTIC AND KINETIC STUDIES

Our previous studies indicated that cobalt macrocycles mediate the photoreduction of CO_2 to CO with *p*-terphenyl (TP) as a photosensitizer and a tertiary amine as a sacrificial electron donor in a 5:1 acetonitrile/methanol mixture.[22] The system enhances the activity of the TP by suppressing the formation of dihydroterphenyl derivatives and produces CO and formate efficiently with only small amounts of H_2. The total quantum yield of CO and formate is 25% at 313 nm in the presence of triethanolamine (TEOA) and $Co(cyclam)^{3+}$.

Transient absorption measurements provide evidence for the sequential formation of the *p*-terphenyl radical anion ($TP^{\bullet-}$), the $CoHMD^+$ complex, the $[CoHMD\text{-}CO_2]^+$ complex and the $[S\text{-}CoHMD(CO_2)]^+$ complex (S = solvent) in the catalytic system containig triethylamine (TEA).[23] The electron-transfer rate constant (k_6) for the reaction of $TP^{\bullet-}$ with $Co^{II}HMD^{2+}$ is 1.1×10^{10} M^{-1} s^{-1} and is probably diffusion controlled because of the large driving force (~ 1.1 V). Flash photolysis studies yield a rate constant (k_7) of 1.7×10^8 M^{-1} s^{-1} and an equilibrium constant of 1.1×10^4 M^{-1} for the binding of CO_2 to $CoHMD^+$. These values are consistent with those previously obtained by conventional methods in CH_3CN.[5]

$$TP^* + TEA \xrightarrow{k_4} TP^{\bullet-} + TEA^+ \qquad (4)$$

$$TP^{\bullet-} + CO_2 \xrightarrow{k_5} TP + CO_2^{\bullet-} \qquad (5)$$

$$TP^{\bullet-} + Co^{II}HMD^{2+} \xrightarrow{k_6} TP + Co^{I}HMD^+ \qquad (6)$$

$$Co^{I}HMD^+ + CO_2 \underset{k_{-7}}{\overset{k_7}{\rightleftharpoons}} Co^{I}HMD(CO_2)^+ \qquad (7)$$

$$Co^{I}HMD(CO_2)^+ + S \underset{k_{-8}}{\overset{k_8}{\rightleftharpoons}} [SCo^{III}HMD(CO_2^{2-})] \qquad (8)$$

$$K_{CO_2} = \frac{[CoHMD - CO_2]}{[Co^{I}HMD^{+}][CO_2]} = \frac{\Delta Abs}{Abs_{\infty}[CO_2]} \quad (9)$$

$$[S\text{-}Co^{III}HMD\text{-}(CO_2^{2-})]^{+} + HA \rightleftharpoons [S\text{-}Co^{III}HMD\text{-}(COOH)^{-}]^{2+} + A^{-} \quad (10)$$

HA = TEA, MeOH, $TEAH^+$

$$[S\text{-}Co^{III}HMD\text{-}(COOH)^{-}]^{2+} + e^{-} \rightarrow Co^{II}HMD^{2+} + CO + OH^{-} \quad (11)$$

e^- = $Co^{I}L^{+}$, $Et_2NC^{\cdot}HCH_3$, $TP^{\cdot -}$

$$OH^{-} + CO_2 \rightleftharpoons HCO_3^{-} \quad (12)$$

The dependence of the decay rate of $TP^{\cdot -}$ on $[CO_2]$ in the absence of the cobalt macrocycle (eq 5) is not linear. We estimate a rate constant $k_5 < 10^6$ M^{-1} s^{-1} for electron transfer between $TP^{\cdot -}$ and $[CO_2]$. This rate constant is consistent with the large reorganization energy of the $CO_2/CO_2^{\cdot -}$ couple (associated the geometry change from a linear to a bent molecule)[24,25] and small driving force for the reaction (0.3 V). Under our photocatalytic conditions the cobalt reacts with the $TP^{\cdot -}$ > 20 times faster than does the CO_2. Thus the direct reduction of CO_2 by $TP^{\cdot -}$ plays a negligible role here and all of the photochemically generated reducing equivalents are captured by the cobalt macrocycle.

The production of CO from $CoL(CO_2)^+$ requires a second reducing equivalent. The source of this equivalent is of interest. Under flash photolysis conditions the $TP^{\cdot -}$ has completely reacted before the $CoL(CO_2)^+$ is formed. On the other hand, under continuous photolysis $TP^{\cdot -}$ can react with the $Co^{II}L^{2+}$ or the $CoL(CO_2)^+$ complexes. In the flash photolysis, where only $Et_2NC^{\cdot}HCH_3$ and/or $Co^{I}L^{+}$ may act as the electron donor, the decomposition of $CoLCO_2^+$ is slow owing to the low concentrations of these two species. In fact, since $CoLCO_2^+$ decomposes faster with low $[CO_2]$ (i.e. higher $[CoL^+]$), CoL^+ is the likely electron donor under flash photolysis conditions. We suggest that reactions 10-12 are responsible for the production of CO in the photolysis. The slow step is likely to be the C–O bond breakage of the bound carboxylic acid with either $Et_2NC^{\cdot}HCH_3$, or $Co^{I}L^{+}$ acting as electron donor. Unfortunately the UV-vis transient spectrum of $[S\text{-}Co^{III}HMD(CO_2^{2-})]^+$ is too weak to study the proton dependence of its disappearance.

4. PHOTOCHEMICAL CO_2 REDUCTION WITH NICKEL MACROCYCLES

4.1 Photochemical CO_2 reduction

In contrast to the cobalt-based system, small amounts of H_2 and no CO are produced when nickel cyclam or other saturated 14-membered tetraazamacrocycles (L) in Figure 3 are used to replace the cobalt complex in the above system.[22] Flash photolysis studies indicate that the electron-transfer rate constant (k_{13}) for the reaction of the *p*-terphenyl radical anion with $Ni^{II}(cyclam)^{2+}$ is 4.3×10^9 M^{-1} s^{-1}. However, when CO_2 is added to the solution, the

decay of the TP anion becomes slower! Flash photolysis studies of the acetonitrile solutions suggest the existence of a minor pathway for $M^{I}L^{+}$ formation that does not involve TP. When TEA (or TEOA) is used with UV excitation (<320 nm), a minor pathway is observed that can be suppressed by the addition of methanol in the case of $CoHMD^{2+}$, but not $Ni(cyclam)^{2+}$.

$$TP^{\cdot-} + Ni^{II}cyclam^{2+} \xrightarrow{k_{13}} TP + Ni^{I}cyclam^{+} \qquad (13)$$

$$Ni^{I}cyclam^{+} + CO_2 \underset{k_{-14}}{\overset{k_{14}}{\rightleftharpoons}} Ni^{I}cyclam(CO_2)^{+} \qquad (14)$$

Both NiL^{+} and $NiL(CO_2)^{+}$ species are formed under CO_2 atmosphere by irradiation at 313 nm in acetonitrile solutions containing TEA and NiL^{2+}. In order to understand the interesting behavior of these nickel-based systems we have studied the nature of the ground-state complexes, electrochemical CO_2 reduction, and the differences in CO_2 binding between cobalt and nickel macrocycles.

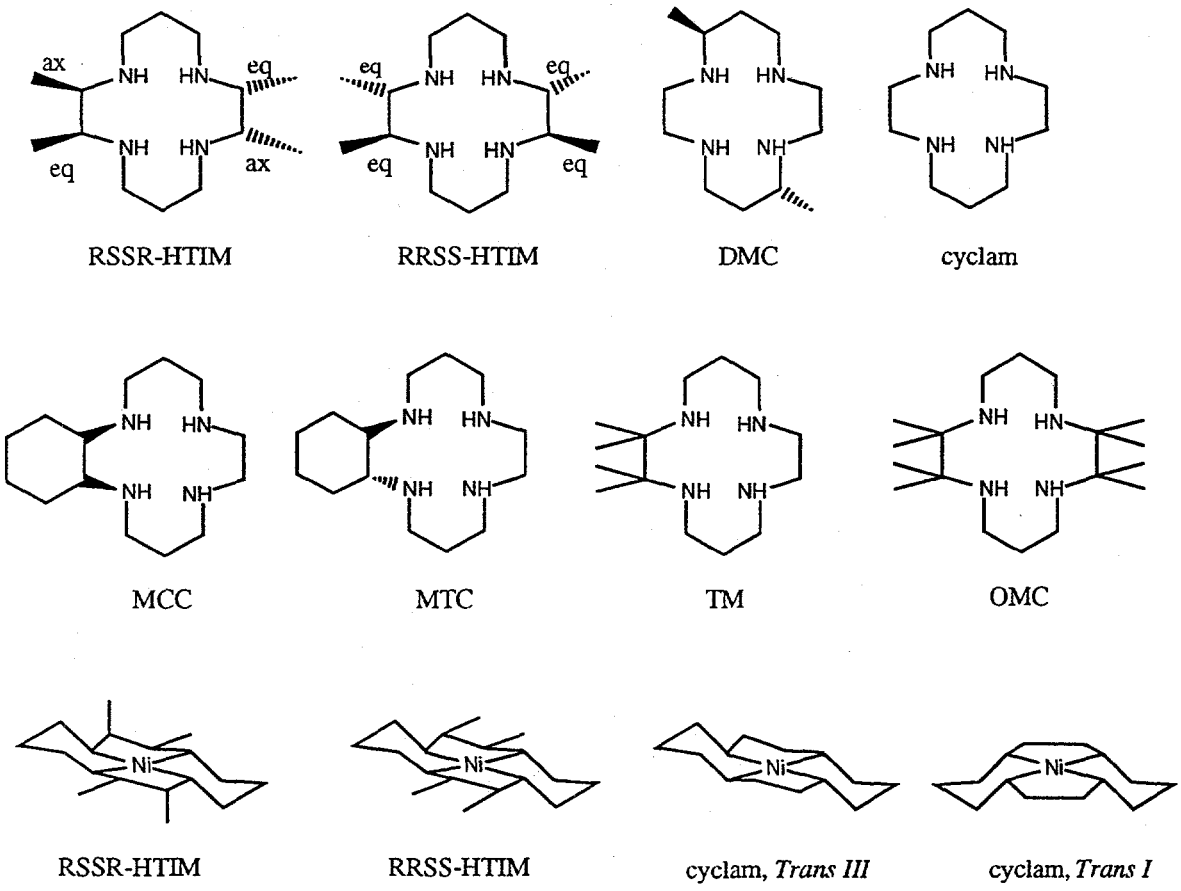

Figure 3. Structures and geometries of metal macrocycles

4.2 Electrochemical CO_2 reduction with nickel macrocycles

The electrocatalytic activity of various nickel macrocycles in aqueous solution were studied. Cyclic voltammograms indicate that *RRSS*-NiHTIM^{2+}, NiMTC^{2+} and NiDMC^{2+} are better catalysts than Ni(cyclam)$^{2+}$ in terms of more positive potentials and/or their larger catalytic currents.[26] Bulk electrolyses with 0.5 mM Ni complexes confirm that these complexes are excellent catalysts for the selective and efficient CO_2 reduction to CO. The macrocycles with equatorial substituents showed increased catalytic activity over those with axial substituents. These structural factors may be important in determining their electrode adsorption and CO_2 binding properties.

4.3 Properties of $Ni^{II}L^{2+}$ complexes

Ni(cyclam)$^{2+}$ is oxidized at 0.98 V and reduced at -1.45 V vs SCE in CH_3CN under argon. Under a CO_2 atmosphere the reduction wave shifts about 10-20 mV more positive, indicating a very small binding constant in CH_3CN. When TEA is added to the solution under argon, the reduction remains at -1.45 V as shown in Figure 4. The oxidation potential is not observed due to the oxidation of TEA. The CV under a CO_2 atmosphere shows a reversible oxidation at 0.31 V. The reduction becomes irreversible and occurs at a very negative potential, -1.8 V in TEA-containing CH_3CN (Figure 4). This indicates that the $[Ni^{I}(TEA)(CO_2)]^{+}$ adduct is unstable. This also explains the slower decay of $TP^{\cdot -}$ under CO_2 atmosphere, since the driving force for electron transfer from the $TP^{\cdot -}$ to $[Ni^{II}(cyclam)]^{2+}$ becomes smaller upon addition of CO_2.

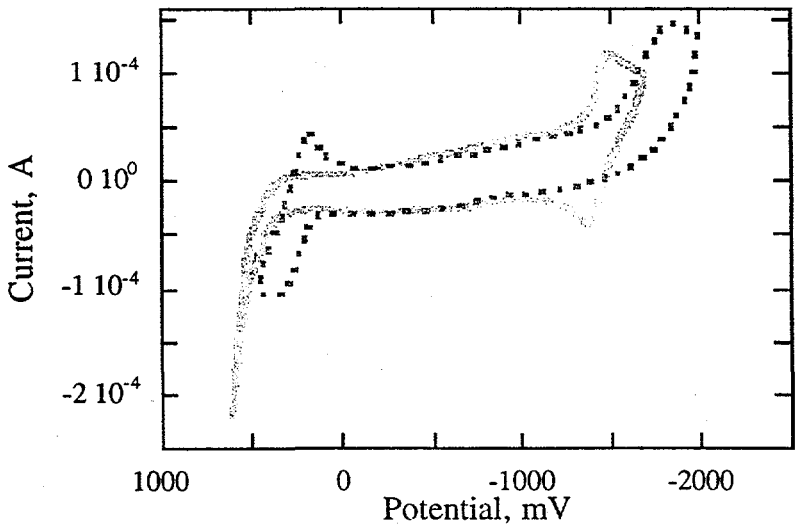

Figure 4. CV for 1 mM Ni(cyclam)$^{2+}$ with TEA under Ar (solid) and CO_2 (dot) in CH_3CN.

The reaction of $Ni^{II}(cyclam)^{2+}$ with TEA/CO_2 was monitored by UV-vis and FT-IR. The d-d absorption intensity of $Ni^{II}(cyclam)^{2+}$ decreases with TEA binding in CH_3CN and shifts to lower energy with CO_2 binding in a TEA-containing CH_3CN solution as shown in Figure 5. Both TEA and CO_2 binding are reversible. The IR spectrum of the $[Ni(cyclam)(TEA)(CO_2)]^{2+}$ adduct indicates two kinds of CO stretching bands at 1615 and 1653 cm^{-1} due to two isomers (*trans I* and *III* in Figure 3). With RRSS-$Ni^{II}HITM^{2+}$, a single isomer, we observed only one CO stretching band at 1630 cm^{-1}. We have determined CO_2 binding constants for both Ni(I) and Ni(II) in CH_3CN. The CO_2 binding constant to Ni(II) cyclam is 1000 M^{-1}, much larger than that of Ni(I). (See below.)

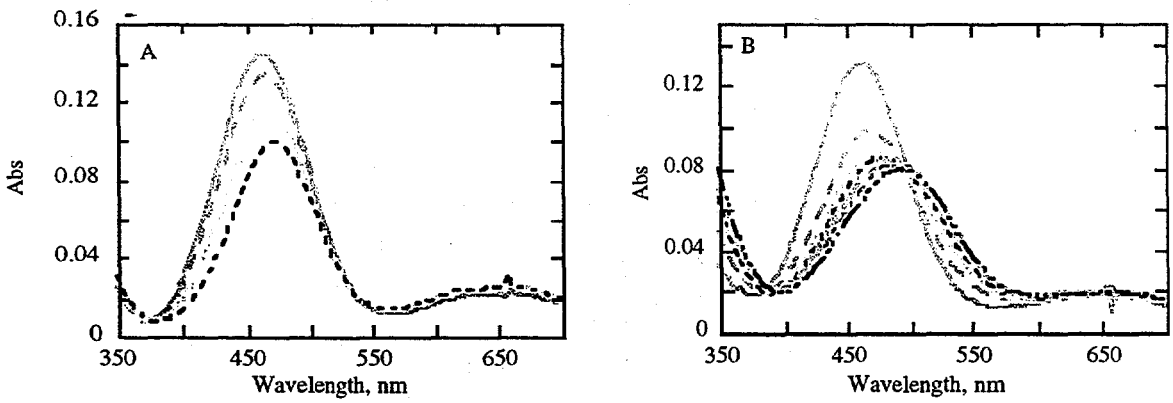

Figure 5. A: Spectral change of $Ni^{II}(cyclam)^{2+}$ by the addition of two equivalent of TEA in CH_3CN.
B: Spectral change of $[Ni^{II}(cyclam)(TEA)_2]^{2+}$ by the addition of CO_2 in a TEA containing CH_3CN.

Table 1 Differences in CO_2 binding and pK_a of $ML(H^-)^{2+}$

	rac-$CoHMD^+$	$Ni(cyclam)^+$	*RRSS*-$NiHTIM^+$	$NiTM^+$
K_{CO_2} in CH_3CN (M^{-1})	1.2×10^4	4	4	< 1
K_{CO_2} in H_2O (M^{-1})	4.5×10^{8a}	11, 16[b]	6.0	< 1
k_{CO_2} in CH_3CN ($M^{-1}s^{-1}$)	1.7×10^8	$\leq 10^7$	$\leq 10^7$	---
k_{CO_2} in H_2O ($M^{-1}s^{-1}$)	1.7×10^{8a}	3.3×10^{7b}	3×10^7	---
pK_a of hydride in H_2O	11.4[a]	1.8[b]	1.9	< 0.5

[a] ref. 11, [b] ref. 28

This behavior was not observed when H_2O was used instead of CH_3CN. $[Ni^{II}(cyclam)]^{2+}$ reacts with both TEA (or OH^-) and CO_2 in H_2O to form a carbonate-bridged dimer, $[(Nicyclam)_2(CO_3)]^{2+}$ (UV-vis: 352, 548 and 900 nm; ν_{CO_2}: 1517, 1460, 1374 cm^{-1}). The structure was confirmed by an X-ray diffraction study.[26]

CO_2 binding constants of Co(I) and Ni(I), and the pK_a of $ML(H^-)^{2+}$ are shown in Table 1. As can be seen, the CO_2 binding constant for $CoHMD^+$ is much larger than those for the Ni macrocycles. In H_2O, the binding constants are larger than the corresponding values in CH_3CN. CO_2 binding constants for Ni macrocycles are very small, however we see some effect due to ligands. Complexes with axial methyl groups, such as NiTM, show almost no binding of CO_2. The trend of the binding constants does not parallel the electrocatalytic activities which is RRSS-$NiHTIM^{2+}$ > $Ni(cyclam)^{2+}$ > $NiTM^{2+}$.[27] The rate constants for CO_2 binding by $CoHMD^{2+}$ are also about 10 times larger than those by Ni macrocycles. The pK_a of cobalt hydride is 11.4, but the corresponding pK_a values for the nickel macrocycles are less than 2.

5. CONCLUDING REMARKS

$CoHMD^{2+}$ and $Co(cyclam)^{2+}$ are good catalysts for photochemical CO_2 reduction because of the small $Co^{II}L^{2+}/Co^{I}L^{+}$ reorganization energy, the fast CO_2 binding to $Co^{I}L^{+}$ (1.7×10^8 M^{-1} s^{-1}) and the large K_{CO_2}. Our XANES results clearly indicate that active metal catalysts, such as $[Co^{I}HMD]^{+}$, can promote two-electron transfer to the bound CO_2 (reduce CO_2 to CO_2^{2-}) and thereby facilitate reduction of CO_2. However since $Co^{I}L^{+}$ reacts with H^+ in CO_2 saturated water (pH ~4) the selectivity of CO_2 reduction in water is not high.

NiL^{2+} (L = cyclam and its derivatives without axial groups) are excellent electrocatalysts for CO_2 reduction. It is known that adsorbed $Ni^{I}L^{+}$ is the active species, however the CO_2 binding constants are not known. We find high selectivity for CO_2 reduction due to the low pK_a of the hydride. $Ni(cyclam)^{2+}$ may not be a good photocatalyst because of the large $Ni^{II}L^{2+}/Ni^{I}L^{+}$ reorganization energy, small CO_2 binding constant to NiL^{+} and instability of the trivalent state. We note that TEA is not an innocent electron donor. It can bind to the nickel center and make the energetics unfavorable for CO_2 reduction. The Ni(I) species is formed by irradiation of the solution containing $[Ni(cyclam)(TEA)_2]^{2+}$ species at 313 nm probably due to the intramolecular electron transfer from TEA to Ni.

ACKNOWLEDGMENT

We thank Drs. Norman Sutin and Carol Creutz for their contribution to earlier work and for their helpful comments. Prof. Rudi van Eldik, Prof. Horst Elias, Prof. Kazuya Kobiro, Ms. Mei Chou, and Dr. David J. Szalda are acknowledged for high pressure work, preparation of $NiHTIM^{2+}$, preparation of $NiTM^{+}$, single crystals of $[(Ni(cyclam))_2(CO_3)]^{2+}$, and its structural determination, respectively. We gratefully acknowledge financial support for travel from the Monbusho International Scientific Program: Joint Research (No.07044148). This research was carried out at Brookhaven National Laboratory under contract DE-AC02-76CH00016 with the U.S. Department of Energy and supported by its Division of Chemical Sciences, Office of Basic Energy Sciences.

REFERENCES

1. Fisher, B. & Eisenberg, R. *J. Am. Chem. Soc.* **102**, 7361 (1980).
2. Tinnemans, A.T.A., Koster, T.P.M., Thewissen, D.H.M.W. & Mackor, A. *Recl. Trav. Chim. Pays. -Bas* **103**, 288 (1984).
3. Beley, M., Collin, J.-P., Ruppert, R. & Sauvage, J.-P. *J. Am. Chem. Soc.* **108**, 7461 (1986).
4. Sutin, N., Creutz, C. & Fujita, E. *Comments Inorg. Chem.* **19**, 67 (1997).
5. Fujita, E., Szalda, D.J., Creutz, C. & Sutin, N. *J. Am. Chem. Soc.* **110**, 4870 (1988).
6. Fujita, E., Creutz, C., Sutin, N. & Szalda, D.J. *J. Am. Chem. Soc.* **113**, 343 (1991).
7. Fujita, E., Creutz, C., Sutin, N. & Brunschwig, B.S. *Inorg. Chem.* **32**, 2657 (1993).
8. Summers, J.S. Ph.D. Thesis , Georgia Institute of Technology, (1989).
9. Fujita, E., Furenlid, L.R. & Renner, M.W. *J. Am. Chem. Soc.* **119**, 4549-4550 (1997).
10. Creutz, C., Schwarz, H.A., Wishart, J.F., Fujita, E. & Sutin, N. *J. Am. Chem. Soc.* **111**, *1153* (1989).
11. Creutz, C., Schwarz, H.A., Wishart, J.F., Fujita, E. & Sutin, N. *J. Am. Chem. Soc.* **113**, 3361 (1991).
12. Schmidt, M.H., Miskelly, G.M. & Lewis, N.S. *J. Am. Chem. Soc.* **112**, 3420 (1990).
13. Golub, G.H. & Kahan, W. *J. SIAM Numer. Anal., Ser. B* **2**, 205 (1965).
14. Hofrichter, J., Henry, E.R., Sommer, J. H., Deutsch, R., Ikeda-Saito, M., Yonetani, T. & Eaton, W. A. *Biochemistry* **24**, 2667 (1985).
15. Shrager, R.I. & Hendler, R.W. *Anal. Chem.* **54**, 1147 (1982).
16. Fujita, E. & van Eldik, R. *Inorg. Chem.* submitted.
17. Manthiram, A., Sarode, P.R., Madhusudan, W.H., Gopalakrishnan, J. & Rao, C.N.R. *J. Phys. Chem.* **84**, 2200 (1980).
18. Wirt, M.D., Kumar, M., Ragsdale, S.W. & Chance, M.R. *J. Am. Chem. Soc.* **115**, 2146 (1993).
19. Wirt, M.D.,Sagi, I., Chen, E., Frisbie, S. M., Lee, R. & Chance, M. R. *J. Am. Chem. Soc.* **113**, 5299-5304 (1991).
20. Sakaki, S. & Dedieu, A. *J. Organomet. Chem.* **314**, C63 (1986).
21. Sakaki, S. & Dedieu, A. *Inorg. Chem.* **26**, 3278 (1987).
22. Matsuoka, S.,Yamamoto, K., Ogata, T., Kusaba, M., Nakashima, N., Fujita, E. & Yanagida, S. *J. Am. Chem. Soc.* **115**, 601-609 (1993).
23. Ogata, T., Yanagida, S., Brunschwig, B.S. & Fujita, E. *J. Am. Chem. Soc.* **117**, 6708 (1995).
24. Ovenall, D.W. & Whiffen, D.H. *Mol. Phys.* **4**, 135 (1961).
25. Chawla, O.P. & Fessenden, R.W. *J. Phys. Chem.* **79**, 2693 (1975).
26 Fujita, E., Chou, M., & Szalda, D.J., to be published.
27. Fujita, E., Haff, J., Sanzenbacher, R. & Elias, H. *Inorg. Chem.* **33**, 4627 (1994).
28 Kelly, C.A., Mulazzani, Q.G., Venturi, M., Blinn, E.L. & Rodgers, M.A.J., *J. Am. Chem. Soc. 117*, 4911 (1995)